Hindawi
Journal of Spectroscopy
Volume 2017, Article ID 8736428, 9 pages
https://doi.org/10.1155/2017/8736428

Research Article

Chemistry and Bioactivity of NeoMTA Plus™ versus MTA Angelus® Root Repair Materials

Sawsan T. Abu Zeid,[1,2] Najlaa M. Alamoudi,[3] Monazah G. Khafagi,[4] and Ensanya A. Abou Neel[5,6,7]

[1]*Endodontic Department, Faculty of Dentistry, King Abdulaziz University, Jeddah, Saudi Arabia*
[2]*Endodontic Department, Faculty of Oral and Dental Medicine, Cairo University, Cairo, Egypt*
[3]*Department of Pediatric Dentistry, Faculty of Dentistry, King Abdulaziz University, Jeddah, Saudi Arabia*
[4]*Spectroscopy Department, Physics Division, National Research Center, Giza, Egypt*
[5]*Department of Operative Dentistry, Faculty of Dentistry, King Abdulaziz University, Jeddah, Saudi Arabia*
[6]*Biomaterials Division, Faculty of Oral and Dental Medicine, Tanta University, Tanta, Egypt*
[7]*Biomaterials and Tissue Engineering Division, UCL Eastman Dental Institute, 256 Gray's Inn Road, London WC1X 8LD, UK*

Correspondence should be addressed to Sawsan T. Abu Zeid; sawsanabuzeid55@hotmail.com

Received 11 February 2017; Revised 13 April 2017; Accepted 20 June 2017; Published 8 October 2017

Academic Editor: Eugen Culea

Objectives. To analyse the chemistry and bioactivity of NeoMTA Plus in comparison with the conventional root repair materials. *Method and Materials.* Unhydrated and hydrated (initial and final sets) materials were analysed by Fourier transform infrared (FTIR) spectroscopy and X-ray diffraction (XRD). For bioactivity study, small holes of dentin discs were filled with either materials, immersed in PBS for 15 days, and analysed with FTIR and scanning electron microscope with energy dispersive X-ray (SEM/EDX). The calculation of crystallinity and carbonate/phosphate (CO_3/PO_4) ratio of surface precipitates (from FTIR) and calcium/phosphate (Ca/P) ratio (from EDX) was statistically analysed using *t*-test or ANOVA, respectively, at 0.05 significance. *Results.* Both materials are tricalcium silicate-based that finally react to be calcium silicate hydrate. NeoMTA Plus has relatively high aluminium and sulfur content, with tantalum oxide as an opacifier instead of zirconium oxide in MTA Angelus. NeoMTA Plus showed better apatite formation, higher crystallinity and Ca/P but lower CO_3/PO_4 ratio than MTA Angelus. SEM showed globular structure with a small particle size in NeoMTA Plus while spherical structure with large particle size in MTA Angelus. *Conclusion.* Due to fast setting, higher crystallinity, and better bioactivity of NeoMTA Plus, it can be used as a pulp and root repair material.

1. Introduction

Mineral trioxide aggregate (MTA) is a hydrophilic calcium silicate-based cement that is traditionally used as a root repair material, mainly developed from Portland cement [1, 2]. It consists of tricalcium and dicalcium silicate particles which harden in a wet environment forming calcium silicate hydrate [2–7]. It proved to be an excellent material for pulp capping, pulpotomy, root perforation repair, root end filling, and pulp regeneration [8]. Difficult manipulation and long setting time, however, limit the use of MTA. New calcium silicate-based, NeoMTA Plus, cement has been recently introduced as fast-set root and periapical tissue repair material. NeoMTA Plus is easily manipulated and remains in place without being washed out (due to its unique gel properties) and does not stain the tooth [9, 10]. Little information, however, is currently available on this material, and its hydration reaction is not yet well understood.

The aim of this study was to examine the chemical composition, surface structure, and bioactivity of the fast-set root repair material, NeoMTA Plus, in comparison with traditional White MTA (MTA Angelus) using Fourier transform infrared (FTIR) spectroscopy, X-ray diffraction (XRD), and scanning electron microscope with energy dispersive X-ray

(SEM/EDX). The null hypothesis of this study is that there is no difference in their composition, surface structure, and bioactivity.

2. Method and Materials

The proposal of this study was accepted by the ethical committee of King Abdulaziz University. White MTA Angelus (Londrina, PR, Brazil) and NeoMTA Plus (Avalon Biomed Inc., Bradenton) were used in this study. The unhydrated dry powder of both materials was analysed with Fourier transform infrared (FTIR 6100, Jasco, Japan) spectroscopy and X-ray diffraction (XRD, Empyrean, Analytical 2010, Holland) to identify their original composition. According to the manufacturer's instructions, each material was mixed with its activator at a powder-to-liquid ratio of 3 : 1. The freshly mixed materials were analysed with FTIR to determine changes during the initial hydration (setting) reaction. Then, the samples were incubated at 37°C and 100% humidity for 24 hours; the final setting was then analysed using the FTIR and XRD.

For bioactivity study, dentin discs of 8 × 8 mm dimension were trimmed from freshly extracted teeth. Using carbide round bur #2 and water coolant, small round holes of 2 mm diameter and 2 mm thickness were prepared. Fresh mix of either of the two investigated materials was packed in the dentin holes (three of each). They were incubated for 7 days at 37°C and 100% humidity to ensure complete setting and then immersed in phosphate buffer solution (PBS) for 15 days. After the immersion period, the dentin discs were splashed with deionized water and air-dried for 24 hours before being analysed with FTIR spectroscopy and scanning electron microscope with energy dispersive X-ray (SEM/EDX, field emission gun, Quanta 250, FEI, Czechoslovakia). From the FTIR spectra, the crystallinity index and carbonate/phosphate (CO_3/PO_4) ratio of the precipitate, formed on the surface of the incubated samples, have been calculated. The crystallinity index (also called infrared splitting factor (IRSF)) was calculated from the sum of heights of v_4 doublet orthophosphate bands at 601 and 557 cm^{-1} divided by the height of the line passing between them [11]; the base line was established between 515 and 630 cm^{-1} (Figure 1). The CO_3/PO_4 ratio has been calculated from the deconvoluted FTIR spectra by dividing the integrated area under the carbonate (v_3CO_3) band at 830–890 cm^{-1} by the integrated area under the phosphate ($v_1v_3PO_4$) band at 900–1200 cm^{-1} [12, 13] (Figure 1). From the EDX data, the calcium/phosphate (Ca/P) ratio of the precipitate formed on the surface of incubated samples was calculated.

For bioactivity, the data of crystallinity index and CO_3/PO_4 ratio were analysed by Student's *t*-test; those of Ca/P ratio were analysed using one-way ANOVA and post hoc test. The statistical analysis was carried at 0.05 significance using SPSS WIN (16.0; SPSS, Munich, Germany).

3. Results

3.1. Fourier Transform Infrared. Generally, the FTIR spectra of both root repair materials are nearly similar but with little variation, indicating the presence of several additives in the powder and liquid components of NeoMTA Plus (Figure 1(a)). *FTIR spectra of unhydrated powders* showed the presence of narrow band of free hydroxyl group of calcium hydroxide at 3642 cm^{-1} [4, 5, 7, 14] and of carbonated group (CO_3) at 1482 cm^{-1} [6, 15, 16]. These peaks are more intense with MTA Angelus. Anhydrate tricalcium silicate (alite) has been also detected at regions 930–915 cm^{-1} [4, 7]; this peak is overlapped with phosphate (β-tricalcium phosphate) [17]. A strong intense band at 883 cm^{-1}, corresponding to CO_3 vibration of calcite [18], which overlapped with HPO_4 band [19], and a peak at ≈750 cm^{-1}, corresponding to tricalcium aluminate [7, 20], have been also detected. A weak band assigned to phosphate group was also detected ≈600 cm^{-1} [4, 19, 21]. An intense band of vibration bending of calcium silicate anhydrate (SiO_4^{2-}) was also seen at 515 cm^{-1} [4, 15, 21] together with weak bands at ≈456 cm^{-1} [22]. Weak bands for the sulfate group (calcium sulfate anhydrate) were detected at 1153 and 661 cm^{-1} [7, 23–25] (Figure 1(a)).

FTIR spectra of liquids of both investigated root repair materials showed the presence of a broad band at ≈3300 cm^{-1} corresponding to the –OH group of water molecules [19, 20, 26]. They also had weak bands at 2900–2800 cm^{-1} assigned to the CH_2 group [14, 27] and bands at 1637 cm^{-1} assigned to the –OH bending mode of absorbed water [17] and overlapped the C = O group [17]. The band at 1637 cm^{-1}, assigned to water molecules, is associated to sulfate (gypsum) phase [5]. The intense band at 1120 cm^{-1}, assigned to v3 vibration of sulfates (SO_4^{2-}) [5, 15, 23], overlapped the band of SiO_4^{2-} vibration [5, 20]. Asymmetric stretching vibration of phosphate (PO_4^{3-}) was identified at 600 cm^{-1} [19, 26]. A weak band at ≈940 cm^{-1}, assigned to symmetric stretching of silicate [17] and overlapping PO_4, was detected in liquid of both materials [17, 28] (Figure 1(a)).

FTIR spectra of hydrated (set) materials (Figures 1(b) and 1(c)) showed the presence of free –OH of calcium hydroxide at 3642 cm^{-1}; this band decreased in initially set while disappeared in completely set materials. The associated –OH of water molecules at 3600–3000 cm^{-1} [5, 6, 21], however, decreased in initially set but become more prominent in completely set materials. The band at 2900–2800 cm^{-1} corresponding to -CH group becomes prominent for hydrated materials [14]. The bands at 1668 cm^{-1} decreased and shifted to ≈1624 cm^{-1} and ≈1600 for NeoMTA Plus and MTA Angelus, respectively. The formation of CO_3 band in the initial set NeoMTA Plus and MTA Angelus has been detected at 1473 and 1498 cm^{-1}; this was also confirmed by the appearance of band at 883 and 871 cm^{-1}, respectively [4, 14, 20, 22, 29]. The former bands have been also shifted to lower frequency (1440 and 1472 cm^{-1}) and become more intense for completely set NeoMTA Plus and MTA Angelus, respectively. The anhydrate calcium silicate of alite and belite phases, detected in initially set materials at ≈940, 515, and 456 cm^{-1} [22], decreased and shifted to 996, 524, and 449 cm^{-1}, respectively. These new bands have been assigned to calcium silicate hydrate (C-S-H) [4, 15, 21, 30]. Sulfate bands at 661 cm^{-1} and phosphate bands at 600 cm^{-1} were

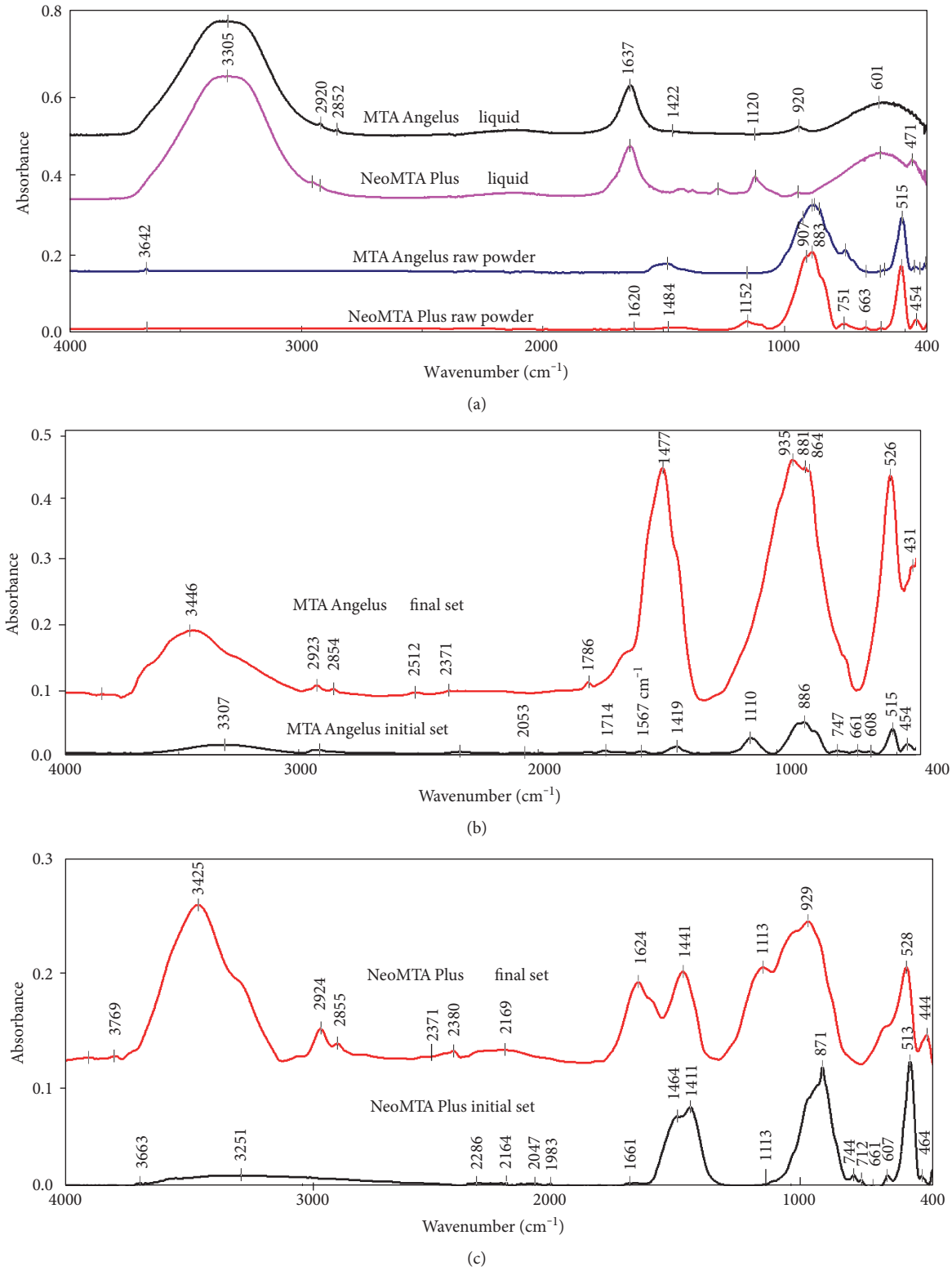

Figure 1: Continued.

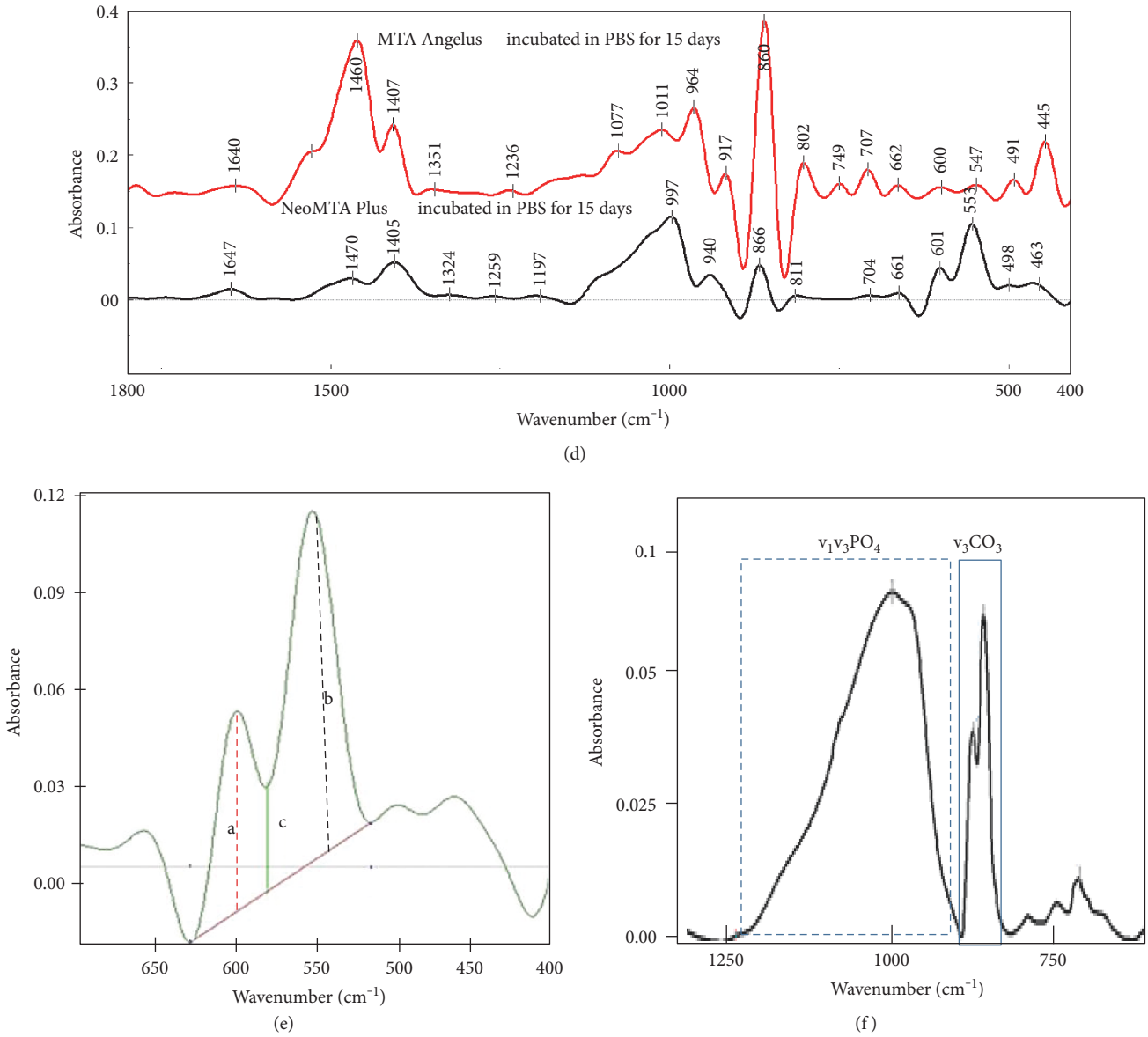

Figure 1: FTIR spectra of (a) original components of MTA Angelus and NeoMTA Plus; completely versus initially set MTA Angelus (b) and NeoMTA Plus (c); deconvoluted spectra of completely set materials that were incubated for 15 days in PBS (d). Crystallinity was calculated by (a + b)/c (e). CO_3/PO_4 ratio was calculated by dividing the area under v_3CO_3 by area under v1v3PO_4 (f).

also shifted to 674 and 640 cm^{-1}, respectively. The calcium sulfate band at 1153 cm^{-1} has been shifted to 1113 cm^{-1} that was assigned to polymerized sulfate in ettringite (hydrated calcium aluminate sulfate) phase [31].

FTIR spectra of hydrated materials incubated in PBS for 15 days (Figure 1(d) showed the presence of overlapped bands at 1800–400 cm^{-1}. Therefore, deconvolution was applied to separate the overlapped bands. Spectra showed the presence of –OH group at 3300–3400 cm^{-1} and carbonated hydroxyapatite (β-type) at 1477 cm^{-1} for MTA Angelus and at 1441 cm^{-1} for NeoMTA Plus [7, 22]. For NeoMTA Plus, bands at 990 cm^{-1} have been assigned to asymmetric stretching vibration of phosphate (PO_4^{3-}) [4], but those at 601 and 557 cm^{-1} were assigned to phosphate bending mode [4, 21, 32]. For MTA Angelus, the band at 964 cm^{-1} was corresponding to phosphate symmetric stretching mode [4] and the band at 445 cm^{-1} has been assigned to SiO_4^{4-} of hydrate silicate gel [4, 7, 21].

After incubation in PBS for 15 days after complete setting, the crystallinity index and CO_3/PO_4 ratio of the precipitate formed on the surface of NeoMTA Plus samples (4.8 ± 0.37 and 0.12 ± 0.01, resp.) were significantly ($P = 0.000$) higher than those recorded for MTA Angelus (3.7 ± 0.52 and 0.52 ± 0.01, resp.).

3.2. X-Ray Diffraction Analysis. XRD analysis for the dry powder of white MTA Angelus root repair shows the presence of tricalcium silicate (alite of hatrurite, $Ca_3(SiO_4)O$; card number: 01-070-8632), calcium sulfate anhydrite ($CaSO_4$; card number: 00-003-0368), calcium carbonate (aragonite,

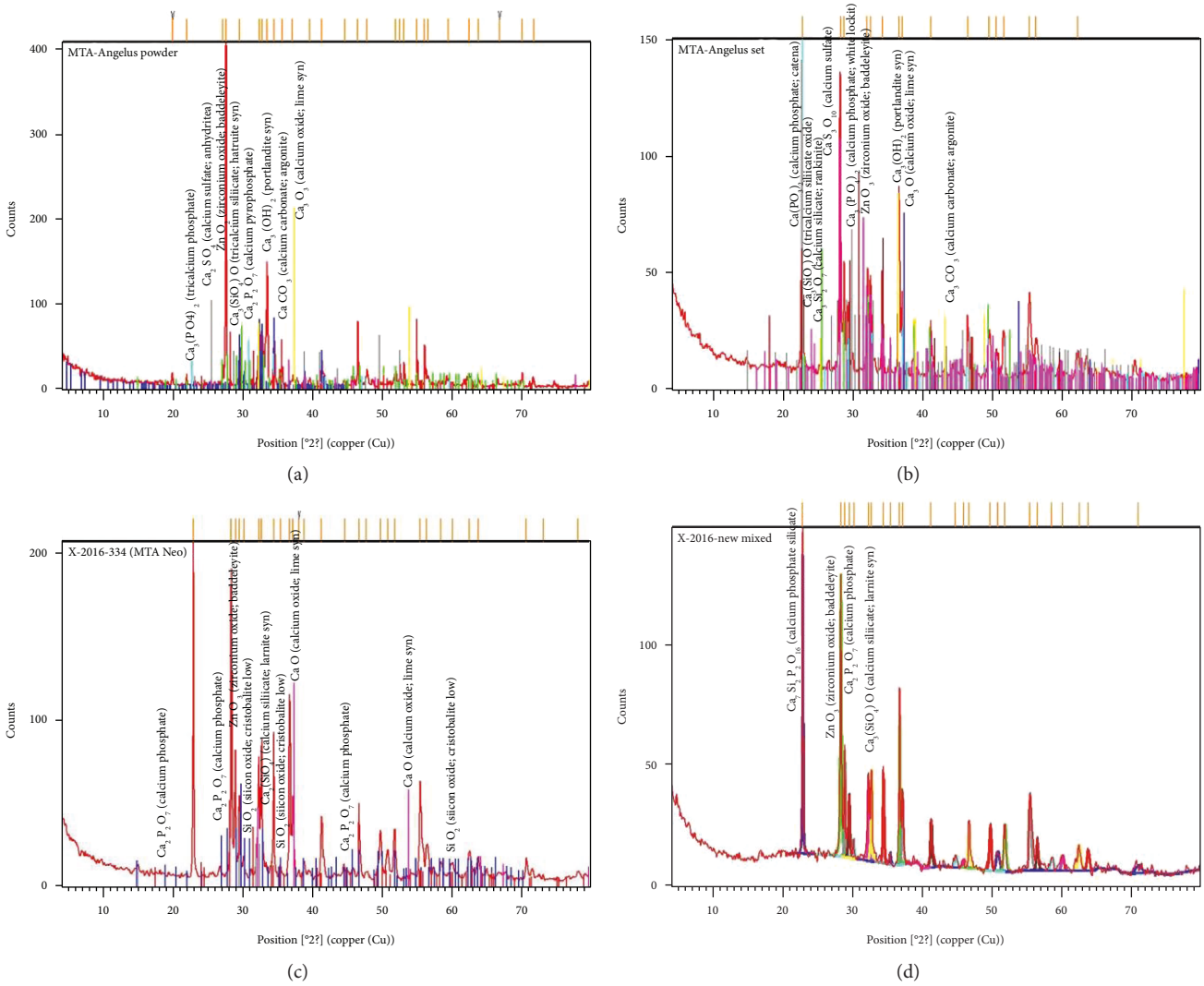

Figure 2: XRD of MTA Angelus powder (a), MTA Angelus hydrated (b), NeoMTA Plus powder (c), and NeoMTA Plus hydrated (d).

$CaCO_3$; card number: 00-003-0893), calcium oxide (lime, CaO; card number: 00-004-0777), calcium hydroxide (portlandite, $Ca(OH)_2$; card number: 01-070-5492), silicon oxide (sristobalite low, SiO_2; card number: 04-008-7818), zirconium oxide (baddeleyite, ZrO_2; card number: 00-024-1165), calcium pyrophosphate ($Ca_2P_2O_7$; card number: 00-002-0647 and 00-003-0605), and tricalcium phosphate ($Ca_3(PO_4)_2$; card number: 00-003-0681) (Figure 2(a)). After setting, calcium silicate (rankinite, $Ca_3Si_2O_7$), tricalcium silicate oxide ($Ca_3(SiO_4)O$; card number: 01-070-1846), calcium hydroxide phosphate (monetite, $CaHPO_4$; card number: 01-070-0359), calcium sulfate (CaS_3O_{10}; card number: 00-021-0166), and calcium phosphate (catena $Ca(PO_3)_2$, card number: 01-079-0700 and Whitelockite β-TCP, $Ca_3(PO_4)_2$; card number: 00-055-0898) phases were detected (Figure 2(b)).

XRD analysis for the dry powder of NeoMTA Plus root repair shows the presence of calcium silicate (hatrurite, Ca_3SiO_5; card number: 98-002-4452), calcium phosphate (α-$Ca_3(PO_4)_2$; card number: 00-029-0359), calcium silicate (tobermorite, $H_{3.5}Ca_{2.25}O_{10}Si_3$; card number: 98-004-0048), tantalum oxide (tantite, β-Ta_2O_5; card number: 01-089-2843), and calcium aluminum oxide ($CaAl_4O_7$) (Figure 2(c)). After setting, calcium silicate hydrate (suolunite, H_2CaO_4Si; card number: 98-008-7951), calcium aluminate oxide (mayenite, $Al_{14}Ca_{12}O_{33}$; card number: 01-076-9897), calcium sulfate ($CaSO_4$; card number: 00-043-0606), and calcium sulfate sulfite ($Ca_3(SO_3)_2SO_4$, card number: 00-038-0701) were also seen in the XRD (Figure 2(d)).

3.3. Scanning Electron Microscopy/Energy Dispersive X-Ray. In scanning electron microscopy images, the surface of hydrated MTA Angelus had spherical as well as needle-like particles (Figure 3(a)). The surface of hydrated NeoMTA Plus showed globular structure of spherical particles that vary from 1 to 3 μm in size (Figure 3(b)). The spherical particles of MTA Angelus were larger in diameter than those observed with NeoMTA Plus. MTA Angelus also showed the presence of more radiopaque phases as indicated by the presence of more contrast on SEM image. Generally, there was no evidence of unreacted powders present in both tested materials (i.e., both materials were completely set).

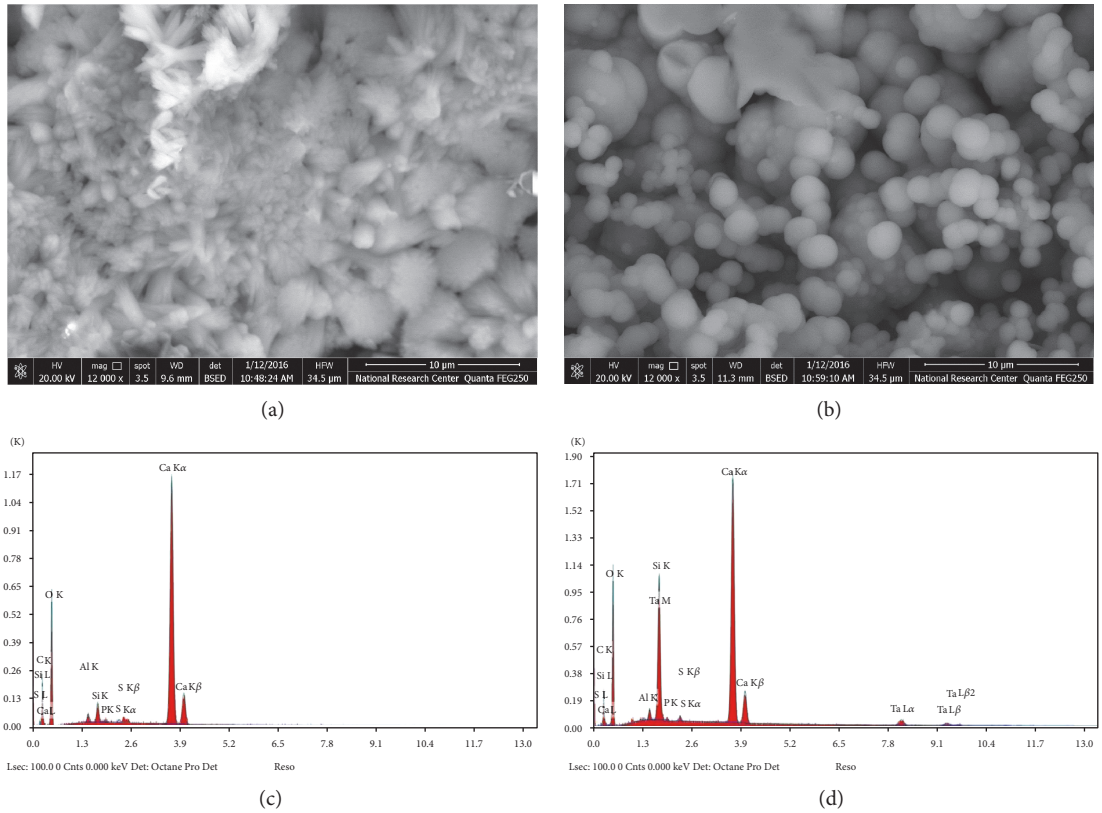

Figure 3: SEM micrographs of complete hydrated samples of MTA Angelus (a) and NeoMTA Plus (b) as well as EDX analysis of hydrated MTA Angelus (c) and NeoMTA Plus (d).

The elemental analysis of hydrated mass of used root repair materials revealed that they were composed mainly of carbon (C), oxygen (O), calcium (Ca), and silicon (Si). The percentage of each element varied between them. Traces of aluminum (Al), sodium (Na), phosphorous (P), and sulfur (S) were also present. Tantalum (Ta) was only detected in NeoMTA Plus (Figures 3(c) and 3(d)). The ANOVA and post hoc tests revealed that there were statistical significant differences between both investigated materials regarding all their constituents ($P = 0.000$) except calcium ($P = 0.53$).

After 15 days of immersing in PBS, the crystals of MTA Angelus and NeoMTA Plus were covered with calcium phosphate precipitates (Figures 4(a) and 4(b)). From the elemental analysis (Figures 4(c) and 4(d)), a significant reduction in C and Si was detected for both materials; Ta was significantly reduced for NeoMTA Plus. P, however, increased. Ca/P ratio was higher in NeoMTA Plus (2.8) than that recorded in MTA Angelus (2.6).

4. Discussion

As seen from FTIR and XRD, both MTA Angelus and NeoMTA Plus are tricalcium silicate-based materials. The opacifier however varies between them (zirconium oxide in MTA Angelus but tantalum oxide in NeoMTA Plus) as detected in XRD. Recently, the biocompatible zirconium or tantalum is added to the root repair materials as radiopacifier instead of barium sulfate to eliminate the coronal tooth discoloration [33]. Other elements as sulfur, indicating the presence of gypsum (calcium sulfate) phase of Portland cement [1], have also been detected from EDX. As indicated from EDX, NeoMTA Plus has higher amount (0.2 ± 0.02) of sulfur than MTA Angelus (0.14 ± 0.01). The presence of gypsum was also confirmed by FTIR; its presence has been detected in both powder and liquid (in particular). During setting reaction, gypsum plays an important role to harden the material as yielding ettringite [31]. It is confirmed in the current study as the band of silicate oxide at $1120\,cm^{-1}$ was dipped and shifted to $1110\,cm^{-1}$ in the initial set spectra and to $996\,cm^{-1}$ in the final set spectra. The changes were related to polymerization of calcium silicate hydrate during hydration reaction [15, 34].

Aluminum was seen in FTIR of unhydrated powder of both materials as well as from EDX and FTIR of both hydrated root repair materials. NeoMTA Plus, however, has higher (0.54) aluminum content than MTA Angelus (0.48). Calcium aluminate oxide (mayenite) has been only detected in XRD of hydrated NeoMTA Plus. The absence of hydrated calcium aluminate from XRD of MTA Angelus could be related to the small size of its crystal or its amorphous nature. Aluminum has a strong effect on setting reaction of MTA; it rapidly reacts with the formed calcium hydroxide in the presence of water forming calcium aluminate hydrate ($4CaO.Al_2O_3.13H_2O$) [1]. Since gypsum and aluminum fasten the setting reaction [1], the presence of gypsum and aluminum in a relatively high amount in NeoMTA Plus could account for its rapid setting [1] as observed during mixing where it sets into a hard mass within few minutes,

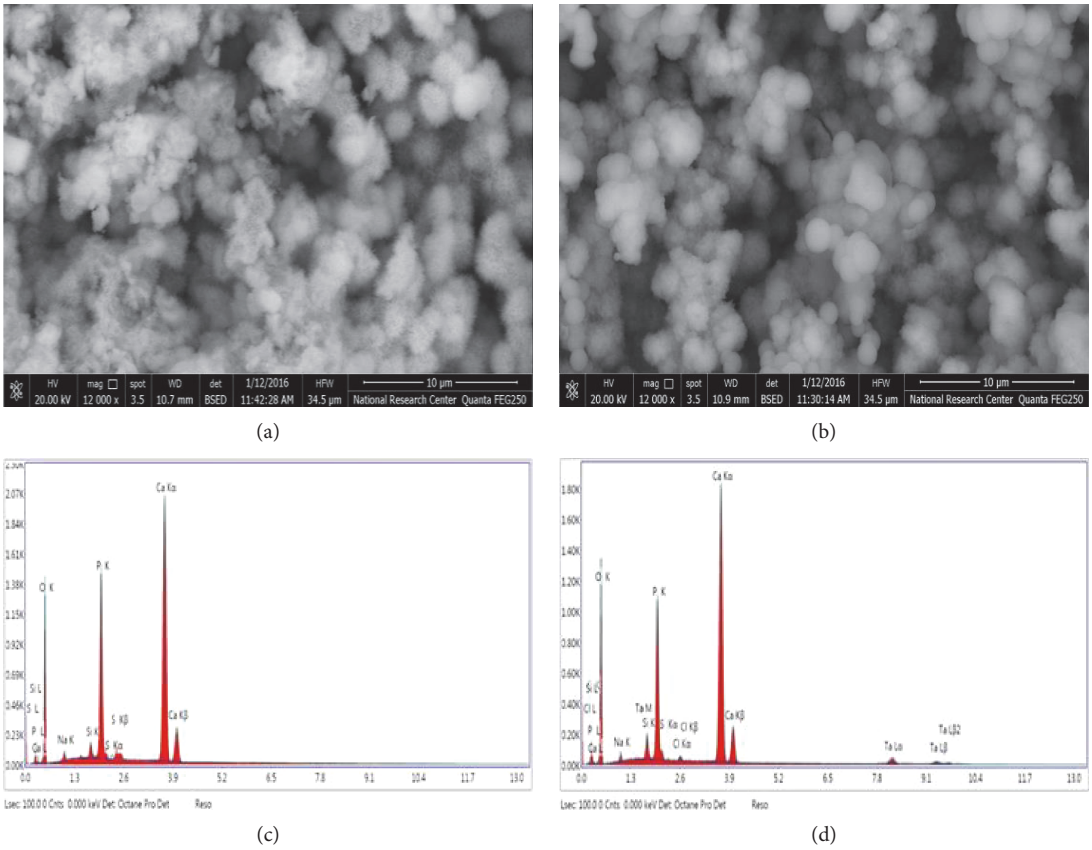

Figure 4: SEM micrographs of hydrated MTA Angelus (a) and NeoMTA Plus (c) after being immersed in PBS for 15 days as well as EDX analysis of hydrated MTA Angelus (c) and NeoMTA Plus (d) after being immersed in PBS for 15 days.

whereas the setting of MTA Angelus could take several hours. After incubation in PBS, aluminum disappeared from EDX analysis of both materials. This could be related to the presence of calcium phosphate precipitates on the surface of materials hiding the trace elements present in the materials' core.

As indicated by FTIR, the investigated root repair materials showed the presence of free –OH (bands at 3642 cm^{-1}) of calcium hydroxide that decreased in initially set materials and disappeared in completely set materials indicating that it has been consumed during the hydration reaction. The associated –OH of water molecules (band at 3600–3000 cm^{-1}) becomes prominent in the spectra of completely set materials indicating the formation of hydrated phases (e.g., calcium hydroxide and calcium silicate hydrate) as the reaction products [5, 6, 21]. Upon hydration, it is not necessary that all tricalcium silicate-based materials produce calcium hydroxide [35]. Even with the presence of free calcium hydroxide as the reaction product, some additives could react with it and hence reduce its amount [36]. In this study, the absence of calcium hydroxide in set MTA Angelus and NeoMTA Plus could indicate that it has been further reacted with the other groups such as phosphate, silicon oxide, or alumina-forming calcium hydroxide phosphate (monetite as in MTA Angelus), more calcium silicate hydrate (in both MTA Angelus and NeoMTA Plus), or calcium aluminate hydrate (as in NeoMTA Plus), respectively. The presence of calcium silicate hydrate was identified in FTIR for both MTA Angelus and NeoMTA Plus, but it is only seen from XRD of NeoMTA Plus. In XRD of MTA Angelus, calcium silicate (rankinite, $Ca_3Si_2O_7$) and tricalcium silicate oxide ($Ca_3(SiO_4)O$) have been detected. This could indicate the amorphous nature of calcium silicate hydrate seen in MTA Angelus.

After incubation in PBS for 15 days, calcium phosphate precipitates were observed on the surface of both MTA Angelus and NeoMTA Plus samples. The Ca/P ratio that was used as an indicator of bioactivity [37] of the precipitates was 2.6 and 2.8 for MTA Angelus and NeoMTA Plus, respectively. These values are close to those observed in a previous study [37]. This high Ca/P ratio indicated that the formed precipitates could be a mixture of hydroxyapatite and may be calcium carbonate (calcite). This finding is also supported by FTIR that confirmed the presence of carbonated hydroxyapatite (β-type) at 1477 and 1441 cm^{-1}, respectively, for both MTA Angelus and NeoMTA Plus samples incubated in PBS for 15 days [7, 22]. The presence of these precipitates indicates that both materials are bioactive [37].

FTIR has been used as a reliable quantitative technique to measure the crystallinity index (a measure of crystal size and perfection) of biological as well as synthetic hydroxyapatite [11, 38, 39]. For this purpose, the splitting of PO_4 vibration bending mode (515–630 cm^{-1}) into doublet bands (v1v3 PO_4) at ≈601 and 557 cm^{-1}, corresponding to the transverse

and longitudinal optical frequency, has been used as an indication of the hydroxyapatite's crystallinity [11, 38, 39]. In amorphous calcium phosphate, due to lattice distortion, PO_4 vibration bending mode is usually seen as a single broad band [39]. The finding of the present study indicated better crystallinity and bigger crystal size of NeoMTA Plus than of MTA Angelus [38]. The crystallinity index of both NeoMTA Plus and MTA Angelus (4.8 ± 0.37 and 3.7 ± 0.52, resp.) falls in the range recorded for synthetic hydroxyapatite (3.6–6.07), but it is generally higher than that recorded for sound human tooth enamel (3.23) [38]. Since the crystallinity increases with increasing Ca/P [39], the high crystallinity of NeoMTA Plus could be correlated with its high Ca/P ratio. The mineral composition of hydroxyapatite however has been measured by investigating the CO_3/PO_4 ratio [11]. The CO_3/PO_4 ratio of NeoMTA Plus and MTA Angelus (0.12 ± 0.01 and 0.52 ± 0.01, resp.) falls in the range recorded for enamel (0.02–0.1) [40]. Increasing carbonate content is associated with a distortion in lattice structure and hence reduces the crystallinity of hydroxyapatite [40]. This could also explain the high crystallinity of NeoMTA Plus obtained in this study.

5. Conclusion

Both root repair materials used in this study, MTA Angelus and NeoMTA Plus, are tricalcium silicate-based materials, but they vary in the opacifier (zirconium oxide in MTA Angelus but tantalum oxide in NeoMTA Plus). NeoMTA Plus, however, has higher sulfur and aluminum content; this could account for its rapid setting compared to MTA Angelus. Upon hydration, tricalcium silicate hydrate has been observed in FTIR of both root repair materials but only in XRD of NeoMTA Plus. The absence of calcium hydroxide in both materials could indicate that it has been further reacted with the other groups such as phosphate, silicon oxide, or alumina-forming calcium hydroxide phosphate (monetite as in MTA Angelus), or more calcium silicate hydrate (in both MTA Angelus and NeoMTA Plus), or calcium aluminate hydrate (as in NeoMTA Plus), respectively. The precipitate formed after incubation in PBS for 15 days has higher crystallinity in NeoMTA Plus samples. This could be related to its high Ca/P but low CO_3/PO_4 ratio. Finally, due to fast setting, higher crystallinity, and better bioactivity of NeoMTA PlusTM, it can be used as an alternative to MTA Angelus as pulp and root repair material.

Conflicts of Interest

The authors declare that there is no conflict of interest with any institution or funding body.

References

[1] T. Dammaschke, H. U. Gerth, H. Zachner, and E. Schafer, "Chemical and physical surface and bulk material characterization of white ProRoot MTA and two Portland cements," *Dental Materials*, vol. 21, no. 8, pp. 731–738, 2005.

[2] M. G. Gandolfi, K. Van Landuyt, P. Taddei, E. Modena, B. Van Meerbeek, and C. Prati, "Environmental scanning electron microscopy connected with energy dispersive x-ray analysis and Raman techniques to study ProRoot mineral trioxide aggregate and calcium silicate cements in wet conditions and in real time," *Journal of Endodontia*, vol. 36, no. 5, pp. 851–857, 2010.

[3] J. Camilleri, F. E. Montesin, L. Di Silvio, and T. R. Pitt Ford, "The chemical constitution and biocompatibility of accelerated Portland cement for endodontic use," *International Endodontic Journal*, vol. 38, no. 11, pp. 834–842, 2005.

[4] M. G. Gandolfi, P. Taddei, A. Tinti, and C. Prati, "Apatite-forming ability (bioactivity) of ProRoot MTA," *International Endodontic Journal*, vol. 43, no. 10, pp. 917–929, 2010.

[5] R. Ylmén, U. Jäglid, B.-M. Steenari, and I. Panas, "Early hydration and setting of Portland cement monitored by IR, SEM and Vicat techniques," *Cement and Concrete Research*, vol. 39, no. 5, pp. 433–439, 2009.

[6] G. Voicu, A. I. Bădănoiu, C. D. Ghițulică, and E. Andronescu, "Sol- gel synthesis of white mineral trioxide aggregate with potential use as biocement," *Digest Journal of Nanomaterials and Biostructures*, vol. 7, no. 4, pp. 1639–1646, 2012.

[7] P. Taddei, E. Modena, A. Tinti, F. Siboni, C. Prati, and M. G. Gandolfi, "Vibrational investigation of calcium-silicate cements for endodontics in simulated body fluids," *Journal of Molecular Structure*, vol. 993, no. 1, pp. 367–375, 2011.

[8] M. Parirokh and M. Torabinejad, "Mineral trioxide aggregate: a comprehensive literature review-part III: clinical applications, drawbacks, and mechanism of action," *Journal of Endodontics*, vol. 36, no. 3, pp. 400–413, 2010.

[9] S. E. Türker, E. Uzunoğlu, and B. Bilgin, "Comparative evaluation of push-out bond strength of neo MTA plus with biodentine and white ProRoot MTA," *Journal of Adhesion Science and Technology*, pp. 1–7, 2016.

[10] J. Camilleri, "Staining potential of neo MTA plus, MTA plus, and biodentine used for pulpotomy procedures," *Journal of Endodontia*, vol. 41, no. 7, pp. 1139–1145, 2015.

[11] M. Lebon, I. Reiche, J. J. Bahain et al., "New parameters for the characterization of diagenetic alterations and heat-induced changes of fossil bone mineral using Fourier transform infrared spectrometry," *Journal of Archaeological Science*, vol. 37, no. 9, pp. 2265–2276, 2010.

[12] C. Rey, B. Collins, T. Goehl, I. Dickson, and M. Glimcher, "The carbonate environment in bone mineral: a resolution-enhanced Fourier transform infrared spectroscopy study," *Calcified Tissue International*, vol. 45, no. 3, pp. 157–164, 1989.

[13] W. Tesch, N. Eidelman, P. Roschger, F. Goldenberg, K. Klaushofer, and P. Fratzl, "Graded microstructure and mechanical properties of human crown dentin," *Calcified Tissue International*, vol. 69, no. 3, pp. 147–157, 2001.

[14] M. J. Blesa, J. L. Miranda, and R. Moliner, "Micro-FTIR study of the blend of humates with calcium hydroxide used to prepare smokeless fuel briquettes," *Vibrational Spectroscopy*, vol. 33, no. 1, pp. 31–35, 2003.

[15] N. B. Singh, S. S. Das, N. P. Singh, and V. N. Dwivedi, "Studies on SCLA composite Portland cement," *Indian Journal of Engineering and Materials Sciences*, vol. 16, no. 6, p. 415, 2009.

[16] A. Santiago and P. Angel, "Calorimetric study of alkaline activation of calcium hydroxide metakaolin solid mixtures," *Cement and Concrete Research*, vol. 31, no. 1, pp. 25–30, 2001.

[17] L. Radev, V. Hristov, I. Michailova, H. M. V. Fernandes, and M. I. M. Salvado, "In vitro bioactivity of biphasic calcium phosphate silicate glass-ceramic in CaO-SiO_2-P_2O_5 system," *Processing and Application of Ceramics*, vol. 4, no. 1, pp. 15–24, 2010.

[18] S. Aparicio, S. B. Doty, N. P. Camacho et al., "Optimal methods for processing mineralized tissues for Fourier transform infrared microspectroscopy," *Calcified Tissue International*, vol. 70, no. 5, pp. 422–429, 2002.

[19] B. C. Liga and B. Natalija, *Research of Calcium Phosphates Using Fourier Transform Infrared Spectroscopy. Book*, INTECH Open Access Publisher, 2012.

[20] J. Madejov and P. Komadel, "Baseline studies of the clay minerals society source clays: infrared methods," *Clays and Clay Minerals*, vol. 49, no. 5, pp. 410–432, 2001.

[21] S. Ahmadi, A. Behnamghader, S. Sharifipoor, and B. Farsadzadeh, "Effect of nano flourhydroxyapatite (nFHA) addition on the acellular bioactivity of MTA cement: an invitro assessment," in *Proceedings of the 4th International Conference on Nanostructures (ICNS4)*, Kish Island, I.R. Iran, 2012; (March):12–14.

[22] G. Voicu, A. I. Badanoiu, E. Andronescu, and C. Bleotu, "Binding properties and biocompatibility of accelerated Portland cement for endodontic use," *Revista de Chimie (Bucharest)*, vol. 63, no. 10, pp. 1031–1034, 2012, http://www.revistadechimie.ro.

[23] M. L. Franquelo, A. Duran, L. K. Herrera, M. C. J. de Haro, and J. L. Perez-Rodriguez, "Comparison between micro-Raman and micro-FTIR spectroscopy techniques for the characterization of pigments from southern Spain cultural heritage," *Journal of Molecular Structure*, vol. 924, pp. 404–412, 2009.

[24] K. I. Zimina, N. A. Filippova, A. G. Siryuk, and G. L. Mashireva, "Study of the infrared absorption spectra of various additive ashes," *Chemistry and Technology of Fuels and Oils*, vol. 6, no. 6, pp. 467–470, 1970.

[25] F. C. Lucia, T. M. David, L. M. Morales, and M. R. Sagrario, *Infrared Spectroscopy in the Analysis of Building and Construction Materials*, INTECH Open Access Publisher.

[26] T. J. Ribeiro, O. J. Lima, E. H. Faria et al., "Sol-gel as methodology to obtain bioactive materials," *Anais da Academia Brasileira de Ciências*, vol. 86, no. 1, pp. 27–36, 2014.

[27] M. R. Sheikh and A. G. Barua, "X-ray diffraction and Fourier transform infrared spectra of the bricks of the Kamakhya temple," *Indian Journal of Pure and Applied Physics*, vol. 51, no. 11, pp. 745–748, 2013.

[28] L. Radev, V. Hristov, I. Michailova, and B. Samuneva, "Sol-gel bioactive glass-ceramics part I: calcium phosphate silicate/wollastonite glass-ceramics," *Central European Journal of Chemistry*, vol. 7, no. 3, pp. 317–321, 2009.

[29] A. Gorassini, P. Calvini, and A. Baldin, "Fourier transform infrared spectroscopy (FTIR) analysis of historic paper documents as a preliminary step for Chemometrical analysis," in *Multivariate Analysis and Chemometry Applied to Environment and Cultural Heritage*, Ventotene Island, Italy, Europe, 2008.

[30] D. Qiu, A. Wang, and Y. Yin, "Characterization and corrosion behavior of hydroxyapatite/zirconia composite coating on NiTi fabricated by electrochemical deposition," *Applied Surface Science*, vol. 257, no. 5, pp. 1774–1778, 2010.

[31] Q. Li and N. Coleman, "The hydration chemistry of ProRoot MTA," *Dental Materials Journal*, vol. 34, no. 4, pp. 458–465, 2015.

[32] M. S. M. Arsad, P. M. Lee, and L. K. Hung, "Synthesis and characterization of hydroxyapatite nanoparticles and b-TCP particles," in *2nd International Conference on Biotechnology and Food Science*, 2011.

[33] I. Khalil, A. Naaman, and J. Camilleri, "Properties of Tricalcium silicate sealers," *Journal of Endodontia*, vol. 42, no. 10, pp. 1529–1535, 2016.

[34] S. Alonso and A. Palomo, "Calorimetric study of alkaline activation of calcium hydroxide±metakaolin solid mixtures," *Cement and Concrete Research*, vol. 31, no. 1, pp. 25–30, 2001.

[35] J. Camilleri, "Hydration characteristics of biodentine and Theracal used as pulp capping materials," *Dental Materials*, vol. 30, no. 7, pp. 709–715, 2014.

[36] J. Camilleri, F. Sorrentino, and D. Damidot, "Characterization of un-hydrated and hydrated BioAggregate™ and MTA angelus™," *Clinical Oral Investigations*, vol. 19, pp. 689–698, 2015.

[37] M. Hosseinzade, R. K. Soflou, A. Valian, and H. Nojehdehian, "Physicochemical properties of MTA, CEM, hydroxyapatite and nanohydroxyapatite-chitosan dental cements," *Biomedical Research*, vol. 27, no. 2, pp. 442–448, 2016.

[38] J. Reyes-Gasga, E. L. Martínez-Piñeiro, G. Rodríguez-Álvarez, G. E. Tiznado-Orozco, R. García-García, and E. F. Brès, "XRD and FTIR crystallinity indices in sound human tooth enamel and synthetic hydroxyapatite," *Materials Science and Engineering: C*, vol. 33, no. 8, pp. 4568–4574, 2013.

[39] G. M. Poralan Jr., J. E. Gambe, E. M. Alcantara, and R. M. Vequizo, "X-ray diffraction and infrared spectroscopy analyses on the crystallinity of engineered biological hydroxyapatite for medical application mater," *The Sciences and Engineering*, vol. 79, no. 1, article 012028, 2015.

[40] C. Xu, R. Reed, J. P. Gorski, Y. Wang, and M. P. Walker, "The distribution of carbonate in enamel and its correlation with structure and mechanical properties," *Journal of Materials Science*, vol. 47, no. 23, pp. 8035–8043, 2012.